THE USE OF HISTOGRAMS FOR DETECTION OF ELECTRICAL INSULATION BREAKDOWN

Jun Wang and Sally M°Inerny

Dept. of Aerospace Engineering and Mechanics
The University of Alabama
P.O. Box 870280
Tuscaloosa, AL 35487

Abstract: Seeded fault experiments were performed on a 50 Hp, 3 phase, 1750 RPM induction motor operated with a variable speed (pulse width modulation, or PWM, type) controller. A hole was cut in the stator housing, allowing access with an industrial heat gun. A single coil of one phase, at the point where it enters the stator laminations, was heated to a series of raised local temperatures. Current and voltage data were simultaneously measured on the target phase and recorded at a sample rate of 2.5 MHz each. Various feature extraction methods were applied to the voltage, current and instantaneous power (voltage times current) time series data. Single point statistics (rms, skewness, and kurtosis), histograms, and Fourier spectra are presented here.

Key Words: Electrical insulation; condition monitoring; variable speed motors.

Introduction: With the development of advanced power electronics and the microprocessor, induction motors for variable speed operation are predominantly fed from pulse width modulation (PWM) inverter drives. Inverter duty induction motors are designed to withstand the rigors of adjustable speed drive (ASD) operation. However, there are significant differences between applications of motors operated on sine-wave power and motors operated on adjustable frequency controls. New PWM drives employing insulated gate bipolar transistors (IGBT) technology offer switching frequencies as high as 20 kHz [1-2], generate steep-front pulses with slopes as high as 6000v/μs, and can induce significant over-voltages [3-4]. Higher switching frequencies result in motor working currents that are more nearly sinusoidal, reduce the audible noise, and are said to offer improved motor efficiencies. However, higher switching frequencies also result in shorter pulse rise times and larger peak over-voltages, subjecting the motor to more severe insulation stresses.

The over voltage induced in PWM operations is unevenly distributed along the coils in a phase. Dr. Bonnett reported that as much as 85% of the peak over-voltage can be dropped across the first turn of the first coil of a phase [5]. This uneven over-voltage distribution causes a significant overstress across the end turns and may result in turn-to-turn insulation failure. The first coil voltage represents the highest possible inter-turn

voltage [4-8] and the shorter pulse the rise time, the greater the voltage dropped across the first coil [9]. For this reason, the focus of our experimental tests was on the first turn of one coil in one phase.

This paper reports preliminary results of research on the development of methods for the early detection of insulation degradation in low voltage (under 600 V) PWM controlled 3-phase induction motors. Voltage and current data were acquired on one phase of a 50 Hp induction motor operating under healthy (baseline) and faulted conditions. The tests were performed at the Motor Test Facility (MTF) at Oak Ridge National laboratories. The results of statistical and spectral analyses of the data are discussed in this paper

Experiments: The availability of 50 Hp drives and the interest of one of the sponsors, ASHRAE, in larger motors led to the selection of a 50 Hp motor as the test item. A new 50 Hp, 440 V, three phase inverter duty motor was donated by Reliance Electric, Inc. Three methods of achieving insulation degradation were considered. Two methods, running the motor at full load with an imbalance and mechanically piercing the insulation in one of the windings, were discussed first. It is difficult to control failures induced by the first of these methods and it could be argued that the second would not be a good representation of normally occurring insulation failure. John Kueck of the MTF suggested removing a section of the motor housing and locally heating a coil. It was decided that this approach would provide the best control and of the three options be the most representative of insulation failures in PWM controlled induction motors.

The end bell of the donated motor was removed and one of the first windings of a phase was identified. Then, a section of the motor housing between the stator laminations and the end bell was cut out in order to expose this coil where it enters the stator, permitting access with an industrial dryer / heat gun. Two type K thermocouples were mounted on the outer edge of the stator laminations roughly half way between the teeth and the motor housing. Only one of the thermocouples worked throughout the tests. Note that the measured temperature provides only limited information on winding temperatures, as it was a local surface temperature. A more complete description of the test plan and instrumentation can be found in Ref. [10].

Test Series One: In the first series of tests, the motor was run until steady state conditions were reached and then the exposed motor coils were heated at the point where they entered the stator coil. Measurements were made using three different PWM switching frequencies and, for each switching frequency, at three different speed and load conditions in the order indicated in Table I.

For each test cycle indicated in Table I, the exposed coil was local heated until the temperature reading stabilized, then data was recorded. The heater was then moved closer to the coil and this process repeated at higher temperatures. Thermocouple readings for the recorded data ranged from 70°C to 252°C with local heating. Preliminary analyses of the data recorded during this set of tests did not show any significant effect of the local heating on the data. A second set of tests performed a month later focused, therefore, on inducing motor failure.

All of the baseline data sets discussed in this paper were recorded during this first series of tests. The baseline test conditions were always: 10 kHz switching frequency, 1750 RPM and 50 Hp. ***Baseline data*** set 1 was recorded before Test Cycle 1; baseline data sets 2 and 3 were recorded between Test Cycles 3 and 4; baseline data set 4 was recorded between Test Cycles 6 and 7; and baseline data set five was recorded after Test Cycle 9.

Table I. Test Series One Operating Conditions.

Test Cycle	Switching Frequency	Motor Speed	HP
1	10k Hz	1750 RPM	50 Hp
2		438 RPM	2.1 Hp
3		875 RPM	7.5 Hp
4	8k Hz	1750 RPM	50 Hp
5		438 RPM	2.1 Hp
6		875 RPM	7.5 Hp
7	2k Hz	1750 RPM	50 Hp
8		438 RPM	2.1 Hp
9		875 RPM	7.5 Hp

Test Series Two: All of these tests were performed with a 10 kHz switching frequency at full speed (1750 RPM) and full load (50 Hp). A more powerful heat gun was purchased and local temperatures were raised much higher than in the previous tests. The following is a brief description of the chronology of the test cycles in this series.

Day One. Two cycles of local heating were performed and then the motor fan intake was partially blocked. With the fan intake partially blocked and no local heating, the thermocouple reading rose to 115°C.

The fan intake blockage was removed and the motor run overnight at full speed and load.

Day Two. The motor fan intake was completely blocked and the motor temperature rose to 130° C. The exposed coil was then locally heated to 360°C while data was recorded.

The locally heated area was allowed to cool, while the global motor temperature continued to rise before the next test cycle. At the start of the next test cycle, the initial temperature reading was 145° C. With local heating in place, the temperature reading reached 383° C. It was ***at the end of this test cycle that Data Set A*** was recorded.

The locally heated area was allowed to cool, while the global motor temperature continued to rise before the next test cycle. At the start of the next test cycle, the initial temperature reading was 158° C. With local heating in place, the temperature reading reached 391° C. It was ***at the end of this test cycle that Data Set B*** was recorded.

The locally heated area was allowed to cool, while the global motor temperature continued to rise before the next test cycle. At the start of the next test cycle, the initial temperature reading was 164° C. With local heating in place, the temperature reading reached 404° C. It was ***at the end of this test cycle that Data Set C*** was recorded.

The fan intake blockage was removed and the motor run overnight at full speed and load.

Day Three. The motor fan intake was fully blocked and thermal insulation was placed between the fins of the motor housing. See Figure 1. Just before local heating of the exposed coils commenced, the thermocouple reading was 152° C. Local heating of the exposed coils was begun, when the thermocouple reading reached 380° C, but before data was recorded ***the motor shut down***.

The motor was restarted and data set D acquired at a thermocouple reading of 158° C with no local heating. Local heating was applied and ***data set E recorded*** at a thermocouple reading of 360° C just as the motor failed for the second and final time.

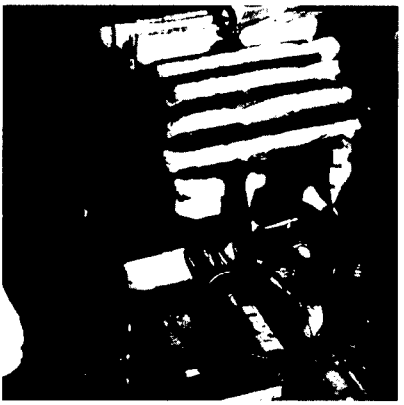

Figure 1. The Motor On the Final Day of Testing. The heat gun is shown directing heat at the exposed coils where they enter the motor stator.

Statistical and Spectral Analyses: A histogram of a given data set can be described as the "frequency of occurrence versus range of values" or "relative frequency of occurrence versus range of values." In either case, the histogram provides information on the probability that the value of a single data point in a set will lie within a specific range of values. Take, for example, a set of 1000 values randomly distributed in the range of -3.5 to 3.5 (normally distributed random numbers generated using the "randn" command in the program MATLAB). When the range is divided into 50 intervals (a.k.a. "bins") and the percentage of the total number of data points whose values lie in each of these ranges is indicated by the height of a bar, one obtains the histogram shown in Figure 2. This relative frequency histogram provides a graphical description of the statistical distribution of the data.

The mean, standard deviation, skewness coefficient and kurtosis coefficient provide simpler single number metrics that can be used to characterize a data set. For a set of N discretely sampled values of $x(t_i)$, these are defined as:

Mean (or Average Value) $$\mu = \frac{1}{N}\sum_{i=1}^{N} x(t_i) \quad (1)$$

Standard Deviation $$\sigma = \sqrt{\frac{1}{N}\sum_{i=1}^{N}(x(t_i)-\mu)^2} \quad (2)$$

Skewness Coefficient $$\gamma_3 = \frac{1}{N}\sum_{i=1}^{N}\frac{(x(t_i)-\mu)^3}{\sigma^3} \quad (3)$$

Kurtosis Coefficient $$\gamma_4 = \frac{1}{N}\sum_{i=1}^{N}\frac{(x(t_i)-\mu)^4}{\sigma^4} \quad (4)$$

For zero mean signals, the standard deviation is the same as the root mean square (or rms) value, x_{rms}. The skewness and kurtosis coefficients are then the third and fourth order moments normalized by the third and fourth power of the rms value, respectively. In this application, the current and voltage are zero mean signals and we will refer to their rms values rather than their standard deviations. In the case of the electrical power (the product of the current and voltage), the mean is the average value and the standard deviation does not have a familiar physical interpretation.

In addition to statistical analyses, Fourier spectra of the voltage, current and power were calculated. The spectra presented in this paper have a resolution of just under 10 Hz and were calculated using a Hanning window and 30 spectral averages with 50% overlap processing.

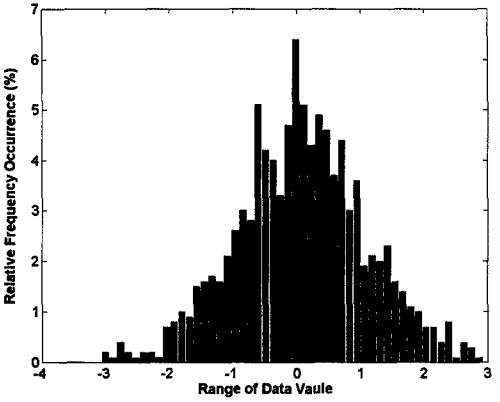

Figure 2. A 50 Bin Histogram of 1000 Numbers Whose Values are Randomly Distributed between –3.5 and 3.5. The numbers were generated in MATLAB using the "randn" command.

Results: Initial comparisons of histograms of the voltage, current and power (voltage times current) time series data indicated dramatic differences between one of the baseline and one of the fault data sets. We later discovered, however, that the differences between different baseline sets were as dramatic as those seen between the baseline and fault data sets. See Figures 3 and 4. It appears that the variability of the histograms even under nominally identical conditions is so large as to mask any variation due to motor health.

A comparison of the single number statistical metrics (mean, rms, maximum value, minimum value, skewness and kurtosis coefficients) between the baseline and fault data sets is provided in Table II. There is no discernible difference in the voltage statistics. As might be expected, the rms current shows a consistent increase. The maximum and the magnitude of the minimum instantaneous current also increase as the motor health degrades. Consistent with the increase in current, the average or mean electrical power also increases.

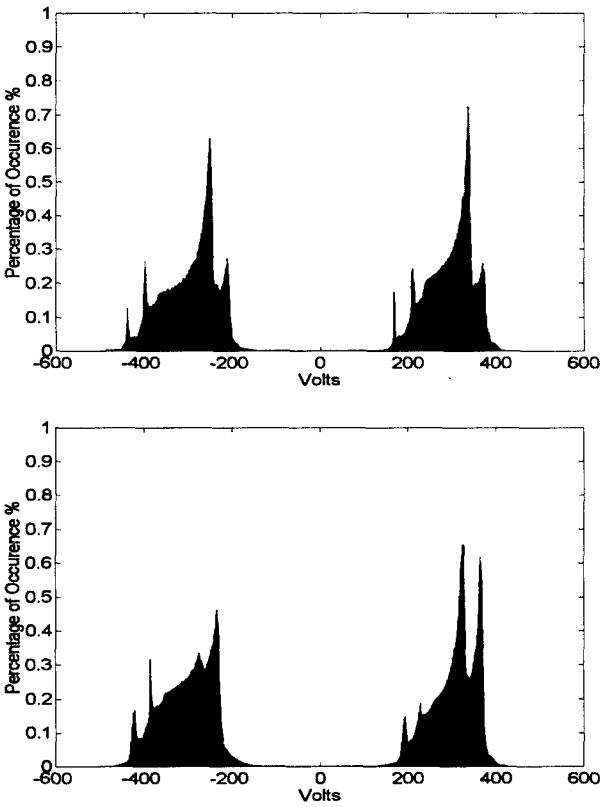

Figure 3. Histograms of Two Baseline Voltage Data Sets: 3 (top) and 4 (bottom).

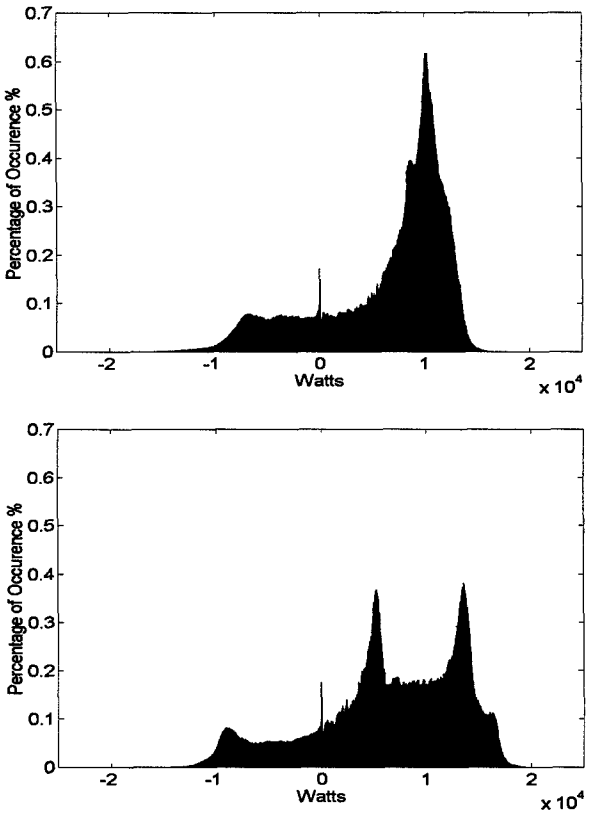

Figure 4. Histograms of Two Baseline Power Data Sets: 4 (top) and 1 (bottom). The peak at 0 Watts was traced to the use of DC coupling of the current signal.

The initial premise of these experiments was that small-scale, local insulation degradation would first be reflected in changes in the high frequency or small-scale data. For this reason, our initial spectral analyses have focused on the full 0-1.25 MHz frequency range, as opposed to the 0-3000 Hz range typically examined in electrical power / motor studies. (Bear in mind that the power consumed by an induction motor is dominated by the motor control frequency, which is 60 Hz here.) Direct comparisons of the voltage spectra of the baseline and fault data sets revealed no discernible differences. Consistent increases in spectral levels were detectable in the current (response) spectra and, consequently, the spectra of the electrical power. Spectral differences occurred primarily in two frequency ranges. For this reason, we adopted an approach that has been used to monitor tail drive shaft bearings in rotor-craft. In this approach, the rms energy in key frequency bands is calculated as a characteristic metric. The frequency ranges we chose were determined by inspection of current spectra, as indicated in Figure 5. The H1 range encompasses a peak

Table II. Single Number Statistical Metrics of Baseline and Fault Data Sets (A-E).

	Baseline Sets	A	B	C	D	E
Starting Motor Temperature	70-81° C	145° C	158° C	161° C	158° C	158° C
With Local Heating	N.A.	383° C	391° C	404° C	N.A.	360° C
V_rms Volts	296.9 to 310.1	297.4	302.0	304.4	305.5	309.7
V_max Volts	463.4 to 478.8	479.5	471.7	473.7	467.4	484.3
V_min Volts	-510.2 to -551.6	-564.3	-496.0	-512.5	-492.3	-529.3
V_kurt coeff	1.123 to 1.146	1.136	1.127	1.141	1.128	1.128
V_skew coeff	-0.0132 to -0.0194	-0.0155	-0.0144	-0.0186	-0.0155	-0.0190
I_rms Amps	**30.4 to 31.2**	**31.7**	**31.6**	**31.3**	**33.2**	**31.5**
I_max Amps	**47.3 to 49.7**	**50.3**	**50.0**	**48.8**	**52.3**	**53.0**
I_min Amps	**-47.0 to -48.8**	**-50.4**	**-49.7**	**-49.2**	**-52.2**	**-53.2**
I_kurt. coeff	1.499 to 1.511	1.512	1.509	1.501	1.501	1.508
I_skew. coeff	0.0053 to 0.0068	0.0054	0.0046	0.0063	0.0051	0.0054
P_max Watts	18640 to 22340	19740	17270	20530	18540	20870
P_min Watts	-16830 to -19730	-23900	-20250	-17430	-20610	-17440
P_mean Watts	**6186 to 6580**	**6674**	**6634**	**6622**	**7032**	**7133**
P_kurt coeff	2.752 to 3.249	3.730	3.702	2.958	3.652	3.190
P_skew coeff	-0.680 to -1.085	-1.115	-1.294	-0.731	-1.290	-1.016

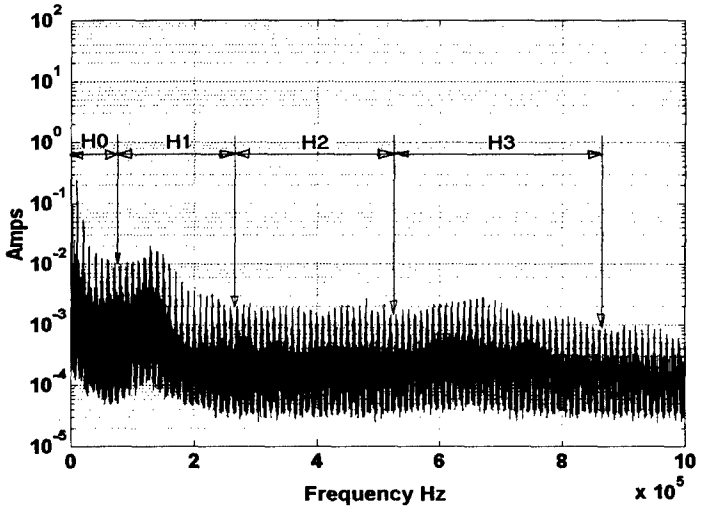

Figure 5. Spectrum of The Current from Baseline Data Set 4 Showing the Frequency Bands Selected for RMS Band Level Calculations.

in spectral levels thought to be a motor resonance effect. Note that the H0 band includes the very low frequency range (0-100 Hz) that dominates the current and electrical power, as can be seen by comparing the results for overall rms level and that in the H0 band in Table III.

The results in Table III confirm what was seen in initial comparisons of the current (and, consequently, electrical power) spectra of the baseline and fault data. Focusing on the high frequency bands not controlled by motor power consumption, the spectral levels in the H1 band (which encompasses what appears to be a motor resonance) are relatively large and show a significant increase with deteriorating motor health. At the low frequency end of the spectrum, the increase in overall (or H0) levels is consistent with the increase in rms current and average power in Table II.

Table III: RMS Current (in Amps) in the Frequency Bands Indicated in Figure 5.

		Baseline Data Sets					Fault Sets				
Frequency Band		**1**	**2**	**3**	**4**	**5**	**A**	**B**	**C**	**D**	**E**
H3	525k – 865 kHz	0.051	0.046	0.045	0.064	0.066	0.088	0.086	0.086	0.091	0.092
H2	265k – 525 kHz	0.049	0.052	0.052	0.052	0.054	0.068	0.068	0.067	0.067	0.067
H1	75k – 265 kHz	0.107	0.080	0.080	0.141	0.146	0.187	0.183	0.182	0.187	0.191
H0	0 - 75 kHz	26.34	27.03	26.99	27.00	26.27	27.48	27.35	27.15	28.72	29.01
Over -all	0 - 1.25 MHz	26.34	27.03	26.99	27.00	26.27	27.48	27.35	27.15	28.72	29.01

Conclusion: The initial intent of the seeded fault tests was to induce localized insulation failure in the first turn of one phase of a three-phase induction motor. The first series of tests raised the local motor temperature in the vicinity of the coil to over 250° C. Preliminary analyses failed to show any significant change in the characteristics of the measured current or voltage. The baseline data sets discussed in this paper were all recorded during this first series of relatively benign seeded fault tests.

The intent of the second series of tests was to induce motor failure by raising both the temperature of the entire motor (blocking the motor fan inlet and placing insulation between the fins of the motor housing) and by local heating of the exposed coils. Five of the data sets recorded during this series of tests were analyzed in this paper. Precise knowledge of the relative motor health at the time that each of these fault data sets was recorded is lacking. It is certain, however, that motor health steadily deteriorated as the tests progressed and the motor was subjected to additional thermal cycles and local heating of the exposed coil.

Statistical and spectral analyses of the recorded baseline and fault data sets were presented. Histograms of the voltage, current and electrical power time series data varied as greatly between baseline data sets as between baseline and fault data sets. No conclusions on motor health could be drawn from visual inspections of the histograms. Single number statistical metrics were also examined. Only the maximum, minimum, and rms values of the current and the mean value of the electrical power showed consistent trends with deteriorating motor health. Spectral analysis confirmed the sensitivity of the current to motor health both in the low frequency band controlled by the motor power consumption (60 Hz, here) as well as in a high frequency band that encompassed a peak in the spectrum attributed to motor resonance.

References

1. Stone, G., Campbell, S., and Tetreault, S., "Inverter-Fed Drives: Which Motor Stators Are at Risk?", *IEEE Industry Applications Magazine*, Sep/Oct 2000, pp. 17-22.
2. Lowery, T.F., "Design considerations for Motors And Variable Speed Drives", *ASHRAE Journal*, Feb. 1999, pp. 28-32.
3. Oliver, J.A., Stone, G.C., "Implications for the Application of Adjustable Speed Drive Electronics to Motor Stator Winding Insulation", *IEEE Electrical Insulation Magazine*, July/Aug. 1995-Vol. 11, No.4, p32-36.
4. Melhorn, C.J., Tang, L., "Transient Effects of PWM Drives on Induction Motors", IEEE Transactions on Industry Applications, vol. 33, No. 4, Jul/Aug. 1997, p1065-1072.
5. Bonnett, A.H., "Analysis of the Impact of Pulse-Width Modulated Inverter voltage Waveforms on AC Induction Motors", IEEE Trans. on Industry Appl. Vol. 32, No.2, Mar/Apr 1996, p 386-392.
6. Sidney B., Jason S., "Will Your Motor Insulation Survive a New Adjustable-Frequency Drive?", IEEE Transactions On Industry Applications, vol. 33. No. 5, Sep/Oct. 1997, p1307-1311.
7. Mbaye, A., Bellomo, J.P., Lebey, T., Oraison, J.M., Peltier, F., "Electrical Stresses Applied to Stator Insulation in Low-Voltage Induction Motors Fed by PWM Drives", IEE Proc. Electr. Power Appl. Vol. 144, No.3, May 1997, p191-198.
8. Oliver, J.A., Stone, G.C., "Implications for the Application of Adjustable Speed Drive Electronics to Motor Stator Winding Insulation", *IEEE Electrical Insulation Magazine*, July/Aug. 1995-Vol. 11, No.4, p32-36.
9. Stone, G., Kapler, J., "The Impact of Adjustable Speed Drive(ASD) Voltage Surges on Motor Stator Windings." *Proceedings of the 1998 IEEE/PCA Cement Industry Technical Conference* May 17-21 1998 Rapid City, SD, p133-138.
10. Wang, J., M^{c}Inerny, and Haskew, T., "Insulation Fault Detection in a PWM Controlled Induction Motor – Experimental Design and Preliminary Results," *Proceedings of the International Conference on Harmonics and Power Quality*, 1-4 October 2000, Orlando, Fl.